Channel bed evolution and sediment transport under declining sand inputs

Karen B. Gran,[1,2] David R. Montgomery,[1] and Diane G. Sutherland[3]

Received 2 June 2005; revised 12 May 2006; accepted 9 June 2006; published 6 October 2006.

[1] Coupled field and laboratory investigations explore links between bed surface structure development and sediment transport as sand inputs decline. On the Pasig-Potrero River, we investigated channel recovery following emplacement of sand-rich pyroclastic deposits in the 1991 eruption of Mount Pinatubo, Philippines. As sediment inputs declined from 1996 to 2003, surface grain size increased, clast structures formed, and sediment mobility and bed load transport rates declined. Our field results parallel those from flume experiments studying highly energetic channels with similar sand contents. As the feed mixture shifted from 70% to 40% sand, surface grain size and gravel interactions increased, forming clusters and armor patches. Bed reorganization into patches initially accommodated coarsening with minimal effect on bed load transport rates, roughness, or friction angle within sandy transport zones. As sand declined further, gravel jams interrupted the connectivity of sandy transport zones, lowering transport rates. Patch development lowered the threshold for the transition from sand-dominated to gravel-dominated transport, focusing this transition over a narrow range of sand content.

Citation: Gran, K. B., D. R. Montgomery, and D. G. Sutherland (2006), Channel bed evolution and sediment transport under declining sand inputs, *Water Resour. Res.*, *42*, W10407, doi:10.1029/2005WR004306.

1. Introduction

[2] Sediment transport in river systems involves important interactions between sand and gravel. When sand content is low, the bed is gravel-dominated, and sand transport depends on mobilization and removal of surface gravels. As the amount of sand increases, it fills the interstices between gravel clasts, eventually leading to sand-dominated transport where gravel clasts move independently over a smooth sand bed. Experimental studies find that sand contents as low as 10–30% enhance gravel transport rates [*Wilcock et al.*, 2001] and affect bed structure and organization [*Ikeda and Iseya*, 1988]. The transition between sand and gravel beds may be characterized by bimodal grain size distributions [*Sambrook Smith and Ferguson*, 1995; *Sambrook Smith*, 1996], grain size patchiness [*Seal and Paola*, 1995], and gravel jams forming in otherwise sand-dominated transport zones [*Ikeda and Iseya*, 1988].

[3] The June 1991 eruption of Mount Pinatubo covered 33% of the Pasig-Potrero watershed area (Figure 1) with loose pyroclastic-flow deposits containing 70–85% sand [*Major et al.*, 1996; *Scott et al.*, 1996]. The abrupt basin-wide increase in sand loading on the previously gravel-bedded Pasig-Potrero River created a smooth, highly mobile, sand-bedded channel. Most gravel bed rivers that experience basin-wide sediment loading [*Gilbert*, 1917; *Knighton*, 1989; *Maita*, 1991; *Madej and Ozaki*, 1996] receive less sand than the disturbed Pasig-Potrero River and may never complete the shift from gravel-bedded to sand-bedded. Because sand loading was so intense, the Pasig-Potrero River is an ideal field site to examine the role of sand on bed development and sediment transport and to observe how highly energetic, sand-rich channels adjust as sand inputs decline. The Pasig-Potrero River is adjusting to a decline in overall sediment supply coupled with a changing sediment mixture as the sand-rich eruptive material is removed and mixed with coarser preeruption deposits.

[4] In this paper we use field surveys of bed and flow characteristics combined with measurements of sediment mobility and transport on the Pasig-Potrero River to examine bed structure development and the associated feedbacks with sediment transport. These measurements and observations are combined with flume experiments modeling highly energetic, sand-rich systems as sand content declines. The initial conditions are based on measurements from the Pasig-Potrero River in 2000–2001, with additional runs designed to emulate future conditions as sand is removed from the system, with sand inputs declining from 70% to 40% of the feed mixture. We examine the role of bed structure development on sediment transport as the bed coarsens and reorganizes, forming discrete coarse patches. These patches accommodate bed coarsening while still maintaining a smooth high-transport zone, minimizing the effect of sand depletion on bed load transport, and restricting the transition from sand- to gravel-dominated transport to a narrow range of sand content. Despite the wide range of grain size mixtures and the changing nature of the bed, we

[1]Department of Earth and Space Sciences, University of Washington, Seattle, Washington, USA.
[2]Now at National Center for Earth-Surface Processes, St. Anthony Falls Laboratory, University of Minnesota, Minneapolis, Minnesota, USA.
[3]Redwood Sciences Laboratory, U.S. Forest Service Pacific Southwest Research Station, Arcata, California, USA.

0043-1397/06/2005WR004306$09.00

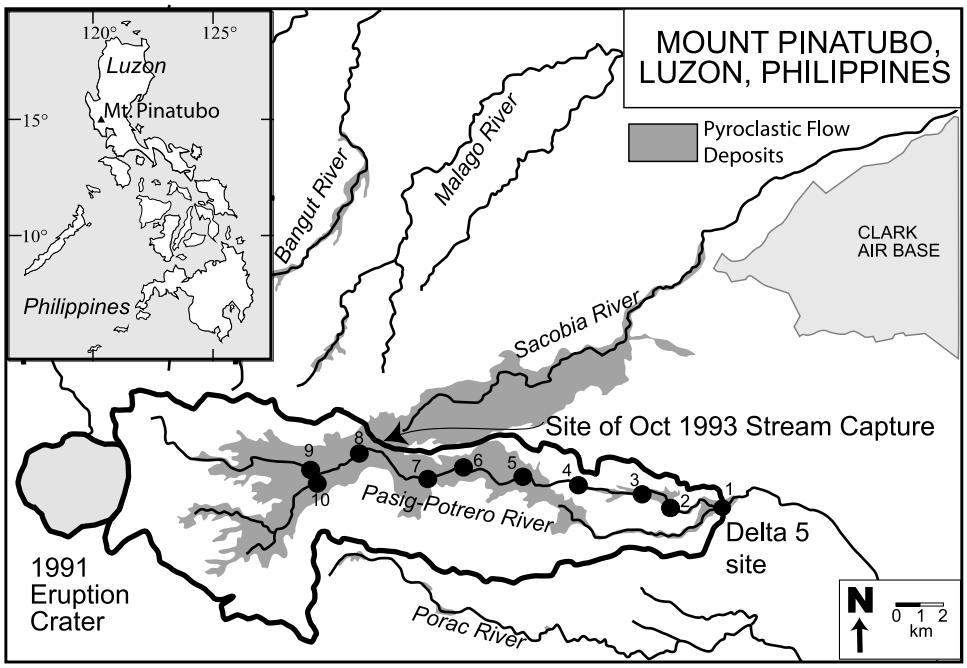

Figure 1. The Pasig-Potrero River drains the east flank of Mount Pinatubo on the island of Luzon, Philippines. Circles denote study sites. Sediment transport was sampled at Delta 5 (site 1) near the alluvial fan head.

found that sediment transport rates were well predicted using a form of the standard *Meyer-Peter and Müller* [1948] transport model for most of our flow conditions.

2. Background

[5] The Pasig-Potrero River offers an ongoing natural experiment on the effects of sand content on bed development and sediment transport, as the river responds to both reductions in sediment supply and changes in the sediment mixture as sandy pyroclastic deposits are removed or stabilized. Experiments have shown that a decrease in sediment supply can lead to surface coarsening, channel narrowing, and/or incision [*Dietrich et al.*, 1989; *Lisle et al.*, 1993]. Because the 1991 pyroclastic flow deposits are predominantly sand, but the preeruption fluvial deposits are predominantly gravel, the ratio of sand to gravel in active transport shifts as pyroclastic material is removed and mixed with preeruption sediment. This decline in sand should affect bed surface structure and sediment transport rates in addition to any effects from a decline in sediment supply.

[6] The role of sand in the transport of sand/gravel mixtures has been the subject of several field studies [*Whiting et al.*, 1988; *Ferguson et al.*, 1989] and experiments [*Iseya and Ikeda*, 1987; *Ikeda and Iseya*, 1988; *Whiting et al.*, 1988; *Wilcock and McArdell*, 1993; *Wilcock et al.*, 2001]. *Ferguson et al.* [1989] measured sediment transport in a bimodal, braided, proglacial stream and found that the channel bed organized into coarse and fine flow-parallel patches, with the majority of the transport moving through fine-grained "sand ribbons." Similar flow-parallel patches observed on the North Fork Toutle River were invoked as a means to enhance transport rates and create rapid downstream fining [*Seal and Paola*, 1995].

[7] In some moderately to poorly sorted beds with both sand and gravel fractions, bed load moves as migrating bed load sheets [*Whiting et al.*, 1988]. In these flow-perpendicular patches, coarse grains detach, move over a transitional zone, and then transport rapidly over a smooth sand bed to the next coarse patch. Transport rates fluctuate greatly during the passage of coarse and fine patches [*Iseya and Ikeda*, 1987; *Kuhnle and Southard*, 1988; *Whiting et al.*, 1988; *Dietrich et al.*, 1989]. Cumulative transport rates reflect rapid transport of gravel in the fine-grained patches [*Iseya and Ikeda*, 1987]. In experiments by *Dietrich et al.* [1987], bed load sheets developed only after adding sand to a fine gravel bed.

[8] *Ikeda and Iseya* [1988] conducted flume experiments with different sand and gravel mixtures, tracking the shift from gravel- to sand-dominated transport as sand content increased. Initially, the bed was gravel-dominated, with sand hidden in the interstices between gravel clasts. Transport rates were thus controlled by mobility of the surface gravel layer, and sand entered into transport through removal of surface gravels. As sand content increased, sand filled the interstices and began forming patches on the surface. Eventually, the bed surface smoothed and transport was sand-dominated with isolated gravel clasts rolling over a sandy bed. Bed load sheets, also called "gravel jams," formed during the transition between gravel- and sand-dominated beds.

[9] Experiments on mixtures with varying sand contents also show an increase in the total sediment transport rate with increasing sand content [*Ikeda and Iseya*, 1988; *Wilcock et al.*, 2001]. An increase in the total transport rate is expected for mixtures with increasing sand content simply because the grain size distribution is finer overall, but transport rates increased as shear stress decreased. In

addition, gravel transport rates increased even as the percentage of gravel in the mixture declined [*Wilcock et al.*, 2001]. *Wilcock et al.* [2001] place the transition between gravel- and sand-dominated transport at 10–30% sand. On the basis of these observations, *Wilcock and Kenworthy* [2002] developed a two-fraction sediment transport model that explicitly accounts for sand content in the bed by incorporating sand content into an incipient motion function.

[10] Nonlinearities in the transport of different mixtures of sand and gravel may influence larger channel morphology, including the relatively common gravel-sand transition that occurs longitudinally rather than temporally. River beds often become finer downstream from abrasion and size selective transport and deposition. In contrast with gradual downstream fining, however, the gravel-sand transition is abrupt, with a decrease of several phi sizes over short distances compared to the overall channel length: 20 km in an 1100 km long channel [*Shaw and Kellerhals*, 1982], 250 m in a 3 km channel [*Yatsu*, 1955; *Sambrook Smith and Ferguson*, 1995], or <1 m in a 21 m laboratory flume [*Paola et al.*, 1992]. The abrupt decline in grain size at the gravel-sand transition has been explained through enhanced abrasion of fine gravels [*Yatsu*, 1955; *Wolcott*, 1988; *Kodama*, 1994], changes in sediment supply [*Knighton*, 1991; *Sambrook Smith and Ferguson*, 1995; *Knighton*, 1999], or changes in local base level [*Pickup*, 1984; *Sambrook Smith and Ferguson*, 1995; *Ferguson*, 2003]. While multiple factors may be involved in different rivers, *Ferguson* [2003] found that the nonlinear effects of interaction between sand and gravel transport coupled with a steadily decreasing slope are enough to trigger an abrupt gravel-sand transition without invoking external forcing like changes in base level or sediment supply.

3. Methodology

3.1. Field Site and Methods

[11] The Pasig-Potrero River drains the east flank of Mount Pinatubo on the island of Luzon, Philippines (Figure 1). In June 1991, Mount Pinatubo erupted, emplacing 5–6 km^3 of pyroclastic flow material on the volcano's flanks, with over 1 km^3 deposited in the Sacobia, Pasig-Potrero, and Abacan basins [*Scott et al.*, 1996; *Daag*, 2003]. Areally, 33% of the Pasig-Potrero basin was covered with valley-filling primary pyroclastic-flow deposits to depths as great as 200 m. The pyroclastic flow material was 70–85% sand by volume [*Scott et al.*, 1996].

[12] The climate at Mount Pinatubo is tropical and monsoonal, with distinct rainy and dry seasons. Intense storms led to the generation of numerous volcanic debris flows and hyperconcentrated flows, referred to collectively as lahars. Sediment yields peaked in 1991, then declined nonlinearly [*Umbal*, 1997; *Tuñgol*, 2002]. In October 1993, the Pasig-Potrero River captured the upper Sacobia River basin, nearly doubling its basin area, from 23 to 45 km^2 [*Daag*, 1994; *Major et al.*, 1996], and generating a second peak in sediment yield in 1994. In 2001, sediment yields at the Delta 5 site at the alluvial fan head (Figure 1, site 1) were still 20 times higher than preeruption levels, and the channel was aggrading ~2 m yr^{-1} [*Gran*, 2005].

[13] Low-flow sediment transport was measured at Delta 5 over a 4-week period during the rainy season in August and September 2001. Discharge fluctuated greatly due to almost daily precipitation events on the volcano. Samples were collected prior to, during, and following daily flood peaks, while conditions were safe. If discharge at the start and end of sampling varied by >30%, the data were discarded.

Table 1a. Flume Parameters

Parameter	Value
Length and width	10 m × 0.7 m
Q_w[a]	9.5×10^{-3} m^3 s^{-1}
Q_s[a]	180 g s^{-1}
Initial slope	0.02
Reynolds number	13,000–20,000
Sand content of runs	70%, 60%, 50%, 40%

[a] Q_w is water discharge, and Q_s is the sediment feed rate.

[14] We sampled both suspended load and bed load using the equal-width increment technique [*Edwards and Glysson*, 1999]. For suspended load, we obtained vertically integrated bulk samples with a U.S. Geological Survey (USGS) DH-48 sampler with a quarter-inch (0.64 cm) opening. Bed load was measured using a handheld modified USGS Elwha pressure-difference sampler with a 200 mm × 100 mm opening and 1 mm mesh bag. All samples were dried, sieved, and weighed in whole phi increments. All sand less than the mesh size (1 mm) was removed from bed load samples: Any sediment <1 mm was considered part of the suspended load fraction, and the DH-48 did sample 1 mm grains in suspension. Bed load transport was computed assuming a 100% sampler efficiency. Sediment transport rating curves were compared with a similar study undertaken by *Hayes et al.* [2002] during the 1997 and 1998 rainy seasons. We also calculated discharge-weighted average particle size distributions for each data set per *Lisle* [1995]. This analysis was limited to overlapping ranges of discharge between the two data sets, thus excluding many high flows measured in 1997.

[15] Sediment mobility was surveyed periodically from 1997 to 2002 at Delta 5 and the Hanging Sabo site, 2.5 km upstream (Figure 1, site 2). We compared grain sizes that remained stable to those in motion in braids up to 25 cm deep, similar to the range of conditions under which bed load samples were collected. Results from these surveys are presented elsewhere in detail [*Montgomery et al.*, 1999; *Gran and Montgomery*, 2005]. We also measured surface grain size distributions and lithologic content using point count surveys [*Wolman*, 1954] at a total of eight additional upstream sites to track changes in the upper basin from 1996 to 2003 in conjunction with the more detailed surveys near the fan head [*Gran and Montgomery*, 2005].

3.2. Experimental Methods

[16] Four experiments designed to study channel development as sand inputs decline were conducted in a 10 m × 0.7 m experimental flume at Humboldt State University (Table 1a). The goal of these experiments was to investigate the role of sand content on bed structure and sediment transport under conditions similar to those on the Pasig-Potrero River. Care was taken to ensure Froude similarity with field conditions and that flow was turbulent (Table 1b).

Table 1b. Flume Versus Field Scaling[a]

	Flume	Field[a]
Slope	0.02–0.04	0.02
Froude number (mean)	1.1–1.6 (1.3)	0.9–1.7 (1.4)
D^*_{50}[b]	0.07 ± 0.04	0.04 ± 0.03
D^*_{84}[b]	0.46 ± 0.11	0.19 ± 0.11
$R_{ep(50)}$[c]	520 ± 470	410 ± 190
$R_{ep(84)}$[c]	7060 ± 2080	4960 ± 4140
Grain size length scale	1	4

[a]Field conditions come from the Pasig-Potrero River at Delta 5 in 2001.
[b]Relative roughness: $D^*_i = D_i/h$.
[c]Explicit particle Reynolds number: $R_{ep(i)} = \sqrt{(\rho_s/\rho_w - 1)gD_i^3}/\nu$.

[17] Initial conditions were based on measurements from the Pasig-Potrero River Delta 5 site in 2001. We kept the grain size distribution as coarse as possible while still ensuring that all grain sizes were mobile. The grain size distribution in the bed started as a 1:4 size ratio of the average subsurface grain size distribution in 2000–2001, with any fraction scaling to <0.25 mm added to the 0.25 mm fraction (Figure 2). This set the composition of the gravel (≥2 mm) and sand (<2 mm) fractions. Adjustments were then made to alter the sand:gravel ratio for each run. The bed and the first run started with a mix of 70% sand and 30% gravel. Water and sediment discharge rates were established such that all size fractions were visibly mobile, with large clasts rolling or sliding downstream over a moving carpet of sand, similar to low-flow conditions on the Pasig-Potrero River.

[18] Bed structure development is a function of both grain size distribution and flow conditions. The relative roughness, $D^*_{50} = D_{50}/h$, where h is flow depth and D_{50} is the median bed load grain size, is a measure of the relationship between grain size and flow depth. It was slightly higher in channels on the Pasig-Potrero River than in the flume (Table 1b). Dimensionless explicit particle Reynolds numbers,

$$R_{ep} = \sqrt{(\rho_s/\rho_w - 1)gD^3}/\nu,$$

were similar for bed load D_{50} clasts in both the field and the flume. Here, ρ_s and ρ_w are sediment and water densities, ν is kinematic viscosity, g is the acceleration due to gravity, and D is the grain size of interest. In the coarse end of the distribution, D^*_{84} and $R_{ep(84)}$ were greater in the flume than in the field, which may have enhanced the influence of the coarsest clasts in our experiments.

[19] We conducted four runs, with 70%, 60%, 50%, and 40% sand content in the feed mix (Table 2). References to each run as the X% run refer specifically to sand content in the feed. The first run (70%) was initialized by screeding a bed composed of 70% sand at a 2% slope. The second (50%) and third (40%) runs began on the bed from the previous run. Following the 40% run, we rescreeded the bed, ran at 70% sand to establish a water-worked surface, and then changed the feed to 60% sand and began the last run. Runs lasted 94 to 140 min.

[20] The 70% run was in dynamic equilibrium with a constant slope and no significant aggradation or degradation. There was no significant coarsening of the bed. Under equilibrium conditions the sediment transport rate should match the feed rate. However, measured transport rates were lower due to sediment losses while changing the sample bag and from splash out of the trap. The initial trap efficiency was estimated at 63%. Improvements to the sediment trap design increased the trap efficiency to an average of 75% for later runs. Sediment transport results were corrected for trap efficiency.

[21] For the other three runs, disequilibrium occurred while the bed aggraded and the slope increased to move sediment of a higher caliber. Equilibrium conditions were met in the 50% and 60% runs as the slope stabilized and bed load distributions and transport rates at the outlet matched feed composition and rates. In the 40% run, slope and sediment transport rates did not stabilize until the end of the run, so it is unclear if dynamic equilibrium was achieved. However, bed load at the outlet did adjust to match the feed distribution within the first 50 min of the run.

[22] During each run we measured water surface elevations and surface velocities. Sediment output was collected, dried, sieved, and weighed to compute transport rates and distributions. Collection frequency varied depending on transport rate, from 25 to 279 s, with an average collection time per run of 78 s. Every 15 min we stopped the run and measured bed elevations along cross sections using a point gage. Every 30 min we scanned the bed topography at 1 mm resolution with a laser scanner and took vertical photographs of the bed. The stoppage of flow clearly affected the bed surface in the 70% run, creating noticeable sand drapes on gravel clasts during the first stoppage of flow. The photos taken at this time were not used for grain size

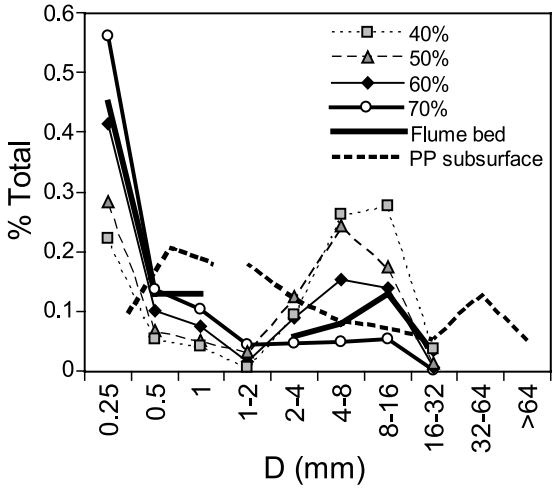

Figure 2. Grain size distributions from the four flume runs and the Delta 5 site on the Pasig-Potrero River. The flume bed was a mix of sieved gravels (binned in 1 phi intervals) and sand from three size fractions (1, 0.5, and 0.25 mm). The flume bed was a 1:4 scale ratio of the Pasig-Potrero River subsurface material. Any fraction that scaled to <0.25 mm was added to the 0.25 mm fraction. Surface distributions were measured through point counts on bed photos taken every 30 min during the course of each run. Sand was lumped together and then plotted here based on the initial composition of sand in the feed. The actual sand content on the bed was likely skewed more toward medium to coarse sand.

Table 2. Basic Flow Conditions for Each Flume Run

	Run Time, min	Average Depth,[a] m	Water Surface Slope[a]	Shear Stress,[b] Pa	Feed D_{50}, φ/mm	Manning's n[c]	
						Full Flume[c]	Transport Zone[c]
70% run	140	0.026	0.021	5.3	0.3/0.8	0.024	0.024
60% run	94	0.034	0.025	8.3	−0.2/1.2	0.034	0.027
50% run	118	0.037	0.027	9.8	−1.0/1.9	0.044	0.023
40% run	129	0.030	0.040	11.8	−1.8/3.6	0.060	0.032

[a]Depth and slope measurements are average values from the portion of the run after equilibrium conditions were met. For the 40% run, we used the last 60 min of run time.
[b]Shear stress was calculated as $\tau = \rho ghS$ using reach-averaged values.
[c]Manning's n roughness was calculated using two different widths: the entire wetted width (full flume) and the width of the transport zone only (transport zone).

analyses. Changes in bed configuration related to flow stoppage were not as noticeable in other runs. Only data in the middle portion of the flume were used in analyses. Water surface slopes and depths were calculated using data between 4 and 8 m (upstream of the outlet). Topographic scans and bed photos were analyzed between 2.75 and 6.75 m, excluding the outer 15 cm on either side of the flume to avoid zones directly affected by roughness elements added to prevent the flow from hugging the walls.

4. Results and Analyses

4.1. Pasig-Potrero River Overview

[23] Observations compiled from 1996 to 2003 indicate that the Pasig-Potrero River is undergoing a transition from a completely unarmored, sand-bedded channel toward a gravel-bedded one [*Gran and Montgomery*, 2005]. As of 2003, gravel-bedded reaches were confined to the upper basin during the dry season. Near the alluvial fan head, pebble clusters and armor patches were prevalent year-round, particularly on low bar complexes and along the edges of major braids.

[24] During the rainy season, braids with widths from a few centimeters to tens of meters actively transported sediment with gravel, cobbles, and boulders rolling or sliding independently over a moving carpet of sand and fine gravel. During low-flow rainy season conditions, average water depths were often <10 cm, yet the flow transported clasts with diameters twice the flow depth [*Montgomery et al.*, 1999; *Gran and Montgomery*, 2005]. Flow was generally supercritical with transient antidunes common. During high-flow events we observed channel-spanning roll waves [*Needham and Merkin*, 1984] 50–100 m wide pulse downstream. Small roll waves 1–5 cm in height occurred during low flow.

[25] Sand and pumice depletion began in the upper basin, extending downstream through time. From 1997 through 2001, average pumice content near the alluvial fan head dropped from 75% to 53%. The bed surface was 39–57% sand. Five kilometers upstream of Delta 5, average pumice content dropped from 83% to 43%, D_{50} increased from 3 to 8 mm, and sand content on the bed surface decreased from 40–50% to 20–30% (Figure 3). Because the primary source for both pumice and sand is the 1991 pyroclastic-flow deposits, we interpret the decline in pumice and sand content to indicate that inputs of eruptive material to the channel network are no longer keeping pace with sediment evacuation. Selective transport is enhancing evacuation of the lighter, finer-grained bedload. Increased mixing of coarser, preeruptive deposits is contributing to the increase in grain size and decrease in pumice in the upper basin. The decrease in pumice has affected overall sediment density in bed load, increasing the density from 1500 kg m^{-3} in 1997 to 2300 kg m^{-3} in 2001.

[26] The effects of surface coarsening were evident as more gravel clasts began to interact, forming clast structures like pebble clusters and armor patches (Figure 4). The increase in sediment density also encouraged formation of more clast structures due to lower overall mobility. On low bar complexes with the highest density of clast structures and armor patches, gravel clasts were able to remain stable under greater flow depths than in major unarmored braids [*Gran and Montgomery*, 2005].

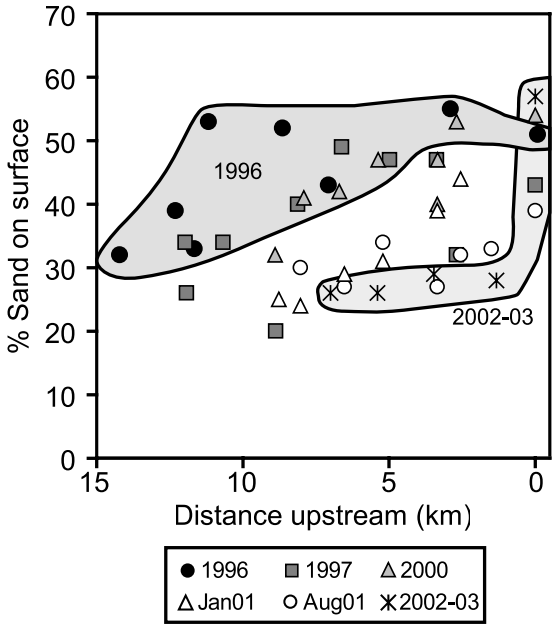

Figure 3. Sand content on the bed surface was measured through point count surveys periodically from 1996 through 2003 on the Pasig-Potrero River, plotted here against distance upstream of the alluvial fan head. The first and last data sets (1996 and 2002–2003) have been shaded to highlight the changes between them.

Figure 4. Stages of bed structure development on the Pasig-Potrero River from (a) unarmored to (b) cluster bed forms to (c) armor patches with sandy transport zones. Gravelometer for scale in Figures 4a and 4b is 340 × 280 mm. The camera mount pole is visible in Figures 4a and 4b.

4.2. Flume Experiments Overview

[27] Under conditions of constant sediment feed rate, the water surface slope, bed slope, and basal shear stress all increased as the percent sand in the feed declined (Table 2). Bed load at the outlet fined during aggradation, although bed surface textures rapidly adjusted to changes in feed distribution. Both the surface grain size and the degree of armoring increased with decreasing sand content (Tables 3a and 3b), and the grain size distribution on the bed surface became increasingly bimodal (Figure 2). Bed surface structure in the form of pebble clusters and armor patches developed as sand declined, but the initial effect on sediment mobility was minimal. Bed partitioning into coarse armor patches and sandy, high-transport zones, along with higher slopes, helped maintain high transport rates despite overall bed coarsening.

4.2.1. Bed Structure

[28] The term "bed structure" refers to the arrangement and sorting of clasts on the channel bed. A bed with structure may exhibit sorting into grain size patches, clustering of coarse clasts into well-defined clast structures like pebble clusters, stone cells, or transverse ribs [*Koster*, 1978; *Brayshaw*, 1984; *Church et al.*, 1998; *Wittenberg*, 2002], or armoring of the bed with respect to the subsurface. Differences in bed structure between runs were visually striking, from unarmored in the 70% run, through cluster-dominated in the 60% run, to armor patches with sand ribbon structure in the 50% and 40% runs (Figure 5). Differences in D_{50}, D_{84}, and D_{90} show the expected trends of increasing grain size with decreasing sand loading, as do ratios of surface to bed load grain size (Tables 3a and 3b). As the sand content declined, the bed coarsened with respect to the bed load.

[29] Figure 5 shows images of the four runs illustrating the development of bed structure. In all runs, the edges of the flume coarsened due to roughness elements placed along the walls. Our discussion here focuses on the middle 0.4 m of the flume. In the 70% run, the flume had an unarmored sand bed with isolated gravel clasts. About half of the gravel present on the bed was arranged into loose clusters. The bed surface had 77% sand cover.

[30] The 60% run was dominated by the formation of pebble clusters, often occupying the entire width of the flume in dense packing. Many of these clusters linked together forming discrete transverse structures 10–15 cm in length. Some clusters joined together to form a weak armor patch next to an open sand ribbon. Surface point count surveys show the bed surface was 60% sand, the same as the sediment feed.

[31] The bed surface in the 50% run developed significant armor patches with a narrow sand ribbon running between them. Sand ribbons occupied 51% of the total bed area, and accommodated most of the sediment transport. In these high-transport zones, the surface was 63% sand, compared with only 31% sand cover on armor patches. Transport in the sand ribbon was primarily sand-dominated, although some gravel jams did form, clogging the otherwise highly mobile transport zone.

[32] In the 40% run, gravel packing on armor patches was dense, with only 18% sand cover, compared with 51% sand in the sandy high-transport zone. Sand ribbons occupied only 43% of the total bed area, and transport there was transitional, with numerous gravel jams.

4.2.2. Friction Angle and Roughness

[33] Initiation of mixed-grain sediment transport is a function of the surface grain-size distribution and bed structure. A clast tends to mobilize in the direction of least resistance, overcoming the lowest angle in the downstream direction, defined as the friction angle, α. Previous studies on water-worked sediments measured α by fixing a bed, placing grains on top of it, and then tilting the bed and tracking when grains mobilize [*Kirchner et al.*, 1990; *Buffington et al.*, 1992]. These studies show a dependence of α on both individual grain size and bed surface grain size distributions. Comparisons between water-worked beds and unworked beds indicate that α increases substantially due to

Table 3a. Surface Grain Size Distributions for Flume Runs

	Sand on Surface, %	Surface D_{50}, φ/mm	Surface D_{84}, φ/mm	Surface D_{90}, φ/mm
70% run	77	0.9/0.5	−0.6/1.5	−2.3/5
60% run	60	0.8/0.6	−3.3/10	−3.8/14
50% run	42	−1.8/3	−3.3/10	−3.7/13
Armor[a]	31	−2.8/7	−3.7/13	−3.9/15
Transport[a]	63	0.8/0.6	−3.1/8	−3.5/11
40% run	32	−2.8/7	−4.0/16	−4.2/18
Armor[a]	18	−3.3/10	−4.0/16	−4.2/18
Transport[a]	51	−0.9/2	−3.5/11	−3.9/15

[a]For the 50% and 40% runs, the bed was subdivided into two zones: armor patches and sandy transport zones. Grain size distributions within each zone were then measured separately.

Table 3b. Bed Load Grain Size Distributions at the Downstream End of the Flume

	Sand in Bed Load, %	Bed Load D_{50}, φ/mm	Bed Load D_{84}, φ/mm	Bed Load D_{90}, φ/mm
70% run	69	−0.5/1.4	−3.5/11	−4.1/17
60% run	59	−1.2/2.3	−4.0/16	−4.1/17
50% run	52	−1.3/2.4	−4.0/16	−4.2/18
40% run	42	−2.3/5.0	−4.1/18	−4.3/19

sorting and organization from flowing water [*Kirchner et al.*, 1990].

[34] Since α is a primary control on the initiation of motion, we investigated how the distribution of α on the bed changes with decreasing sand content and increasing bed structure. We measured a proxy for friction angle, α', using the scanned bed topography to determine the angle a clast needs to overcome to mobilize downstream. At each pixel, we calculated the slope of a small wedge facing downstream, fit to the measured topography. Here we present results from a wedge 9 mm long, with a span of 36° (Table 4). Distributions of positive α' for each run are given in Figure 6. They show a dramatic increase in α' as sand content decreased. Because most of the transport was confined to the fine-grained sand ribbon running between armored patches in the 50% and 40% runs, we recalculated α' in each zone. The mean α' for transport zones were substantially lower than α' for the entire bed (Table 4).

[35] Roughness was computed as Manning's n using reach-averaged quantities. Roughness increased from 0.024 to 0.06 from the 70% to the 40% run. However, because most of the flow and sediment transport was confined to the sand ribbon, we recomputed roughness within the sand ribbon for the 40% and 50% runs. Roughness in these high-transport zones changed little between runs, varying from 0.024 to 0.032 (Table 2).

4.3. Sediment Transport

[36] Rainy season low-flow suspended load and bed load transport data from the Pasig-Potrero River in summer 2001 were compared with 1997–1998 transport data [*Hayes et al.*, 2002]. All suspended load samples in 2001 had con-

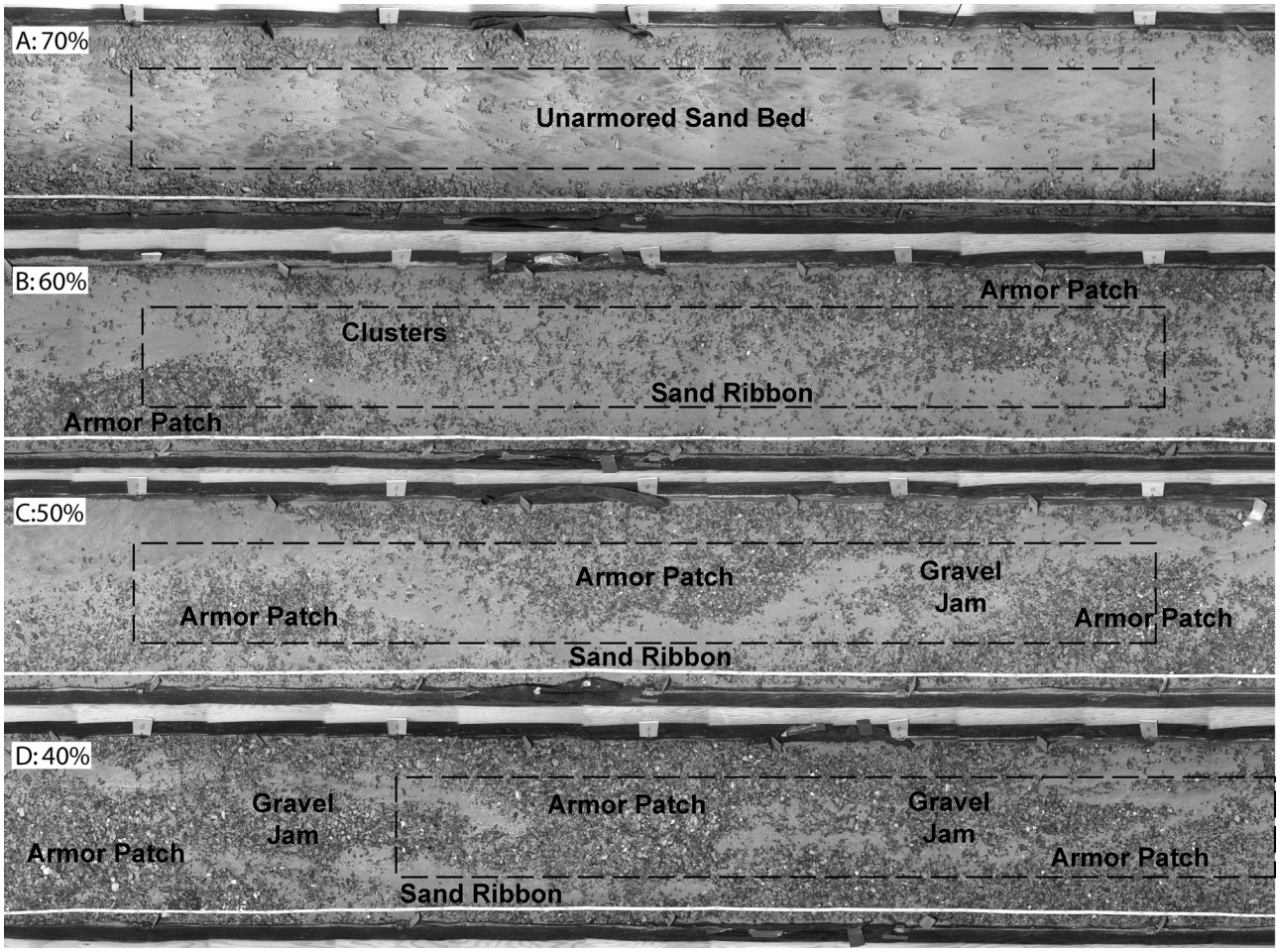

Figure 5. Photographs of the bed surface during each of four flume runs with different feed mixtures: (a) 70% sand, (b) 60% sand, (c) 50% sand, and (d) 40% sand. The dashed boxes denote study patches for photo and topographic scan analyses. The bed progressed from sandy and unarmored with isolated gravel clasts and few clusters (Figure 5a) to mostly clustered over sand bed with a few weak armor patches (Figure 5b) to structured with armor patches and a highly mobile sand ribbon (Figures 5c and 5d). In Figure 5d, large gravel jams can be seen in the otherwise sandy transport zone between armor patches.

Table 4. Average α' for Each Run[a]

	70% Run	60% Run	50% Run	40% Run
Total bed	21.9	39.4	48.4	55.2
Armor patches			56.3	60.2
Sandy transport zones			39.3	47.4

[a]Values given in degrees.

centrations (0.1–3.4% sediment by weight) well below the threshold for hyperconcentrated flow of 40% sediment by weight [*Beverage and Culbertson*, 1964]. In 1998, *Hayes* [1999] measured two storm events with peak discharge concentrations that were close, but all other low-flow measurements were well below hyperconcentrated flow levels (0.9–8.4% sediment by weight). There was little change in low-flow suspended load concentrations from 1997 to 2001, so a single suspended load rating curve (R^2 = 0.68, n = 92) can describe both data sets:

$$C = 12.0 \times Q_w^{0.70}, \quad (1)$$

where C is the concentration (kg m^{-3}) and Q_w is the water discharge (m^3 s^{-1}) (Figure 7a). This curve excludes data with Q_w < 1 m^3 s^{-1}, collected primarily from individual braids in 2001. Below this discharge, there is a kink in the curve, and concentrations have considerable scatter.

[37] Bed load made up an average of 38% (±15%) of the total load (suspended load plus bed load). Comparing samples collected over the same range of unit discharges ($0.05 < q_w < 2.0$ m^2 s^{-1}), we found no significant changes in discharge-weighted grain-size distributions of low-flow bed load between 1997–1998 and 2001. We do not have bed load samples taken during large storm events to compare between years.

[38] Rating curves comparing low-flow volumetric bed load discharge, Q_b, were developed for 2001 and compared with data from 1997–1998 [*Hayes et al.*, 2002]. In both years, a similar volume of sediment could be moved by the same discharge of water, and thus the data can be described by a single linear rating curve (R^2 = 0.85, n = 78) (Figure 7b):

$$Q_b = 0.0043 \times Q_w. \quad (2)$$

Unit volumetric bed load transport, q_b, rating curves are similar (R^2 = 0.69, n = 78):

$$q_b = 0.0042 \times q_w. \quad (3)$$

Although the same volume of sediment was transported for a given flow from 1997 through 2001, the mass transported actually decreased because the average sediment density increased from 1500 kg s^{-1} in 1997 to 2300 kg s^{-1} in 2001. A dimensionless approach is able to incorporate the changing sediment density, so we computed a dimensionless unit bed load transport rate, q_b^*:

$$q_b^* = \frac{q_b}{\rho_s \sqrt{\mathrm{R} g D^3}} \quad (4)$$

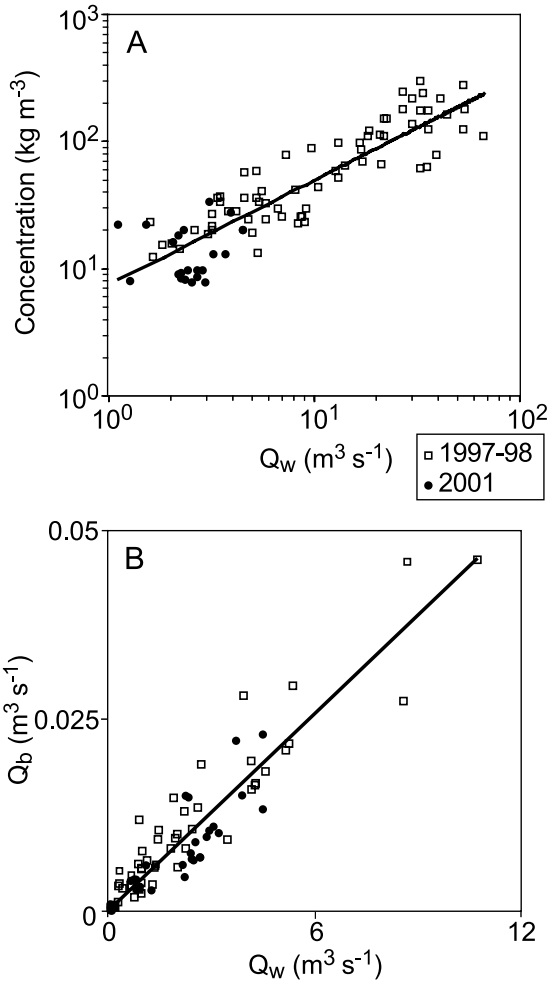

Figure 7. Sediment transport rating curves developed on the Pasig-Potrero River from data in 1997–1998 [*Hayes*, 1999; *Hayes et al.*, 2002] and 2001 (this study) including (a) suspended load and (b) bed load. Concentration data in Figure 7a are truncated at Q_w = 1 m^3 s^{-1}.

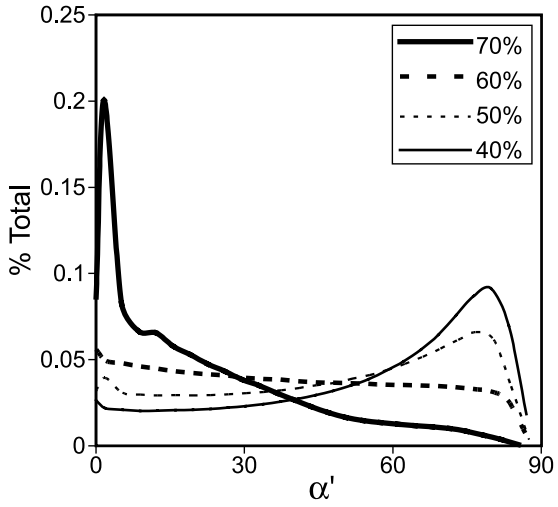

Figure 6. Histogram plots of friction angles (measured here as a proxy, α') for each of the four flume runs. Overall, α' were much lower in the high sand runs, and increased as sand content declined.

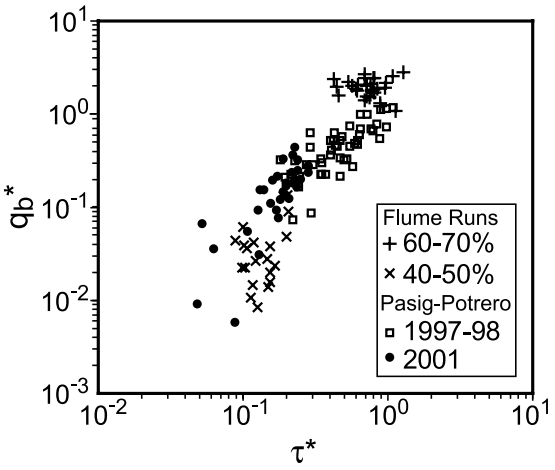

Figure 8. Dimensionless bed load (q_b^*) versus dimensionless shear stress (τ^*) on the Pasig-Potrero River in 1997–1998 [*Hayes*, 1999; *Hayes et al.*, 2002] and 2001 and from all four flume runs. Transport data from the field plot along the same curve, but there is a shift from 1997–1998 to 2001. Transport data from the flume span the range of conditions measured on the Pasig-Potrero River, separating into two zones based on sand content in the feed (40–50% sand and 60–70% sand).

and a dimensionless shear stress, τ^*:

$$\tau_b^* = \frac{\tau_b}{\rho_w \mathsf{R} g D}, \tag{5}$$

where τ_b is the basal shear stress, $\mathsf{R} = (\rho_s - \rho_w)\rho_w$, and $D = D_{50}$. The data collapse to a single, nearly linear curve, but there is a shift from 1997–1998 to 2001 primarily resulting from the increase in sediment density (Figure 8).

[39] In the experimental runs, water surface slope increased with decreasing sand content, increasing τ_b (Table 2). We computed τ^* and q_b^* using transport data from the portion of each run at equilibrium (Figure 8). For the 40% run, we used data collected in the last 60 min, although it was unclear if equilibrium was achieved. The flume data span the range of conditions measured on the Pasig-Potrero River from 1997 through 2001 and cluster into two distinct groups based on sand content.

[40] Because our system is not supply-limited, transport rates should be well modeled by existing sediment transport models; however, the wide range of sediment mixtures could prove challenging for models designed for specific types of rivers. Our sediment is a bimodal mixture, so we chose a surface-based two-phase model designed for mixtures by *Wilcock and Kenworthy* [2002] (WK). The WK surface-based model predicts bed load transport rates for gravel and sand fractions independently, based on the median grain size of each mode and the proportion of sand in the bed surface. The sand content on the bed surface (F_s) in our runs ranged from 0.32 to 0.77, mostly above the range of influence of the sand-gravel transition in the WK model (~30% sand). The reference shear stress values for sand (τ_{rs}^*) and gravel (τ_{rg}^*) fractions are thus at or close to the limiting values found in high sand environments ($\tau_{rs}^* = 0.065$; $\tau_{rg}^* = 0.011$). These τ_{ri}^* values represent the τ_b at which transport rates reach a small reference value ($W_i^* = 0.002$), i refers to the fraction (sand or gravel), and W^* is a dimensionless sediment transport rate (see *Wilcock and Kenworthy* [2002] for a full explanation of the model).

[41] Sand and gravel transport rates were calculated independently, then summed together and nondimensionlized using equation (4) (Figure 9). The results are compared visually (Figure 9) and by comparing the average difference, λ, between the $\log_{10}$ of predicted and measured transport rates: $\lambda = \log_{10} q_{b(pred)} - \log_{10} q_{b(meas)}$ (Figure 10). With the exception of the 70% run, most of the transport rates were overpredicted (field: $\lambda = 0.8 \pm 0.3$; flume: $\lambda = 0.2 \pm 0.4$). A breakdown of gravel and sand transport rates found that gravel transport rates were underpredicted in the 70% sand run by an order of magnitude ($\lambda = -1.0 \pm 0.4$), but because gravel transport was a small fraction of the total transport, total transport rates were well-predicted. However, for the other three runs, gravel was well-predicted ($\lambda = -0.1 \pm 0.7$) and sand was overpredicted ($\lambda = 0.7 \pm 0.4$), leading to an overprediction of total transport rates.

[42] The effectiveness of the WK model was compared with two additional sediment transport models, the classic *Meyer-Peter and Müller* [1948] (MPM) and *Engelund and Hansen* [1967] (EH) models designed for uniform-size sediment transport in the absence of bed forms. The EH model, $q_s^* = (0.05/C_f)(\tau^*)^{5/2}$, relies on a coefficient of friction, C_f, determined from flow hydraulics, while the MPM model uses a critical shear stress, τ_c^*, determined from the median grain size, D_{50}. The original MPM model has been updated by *Fernandez-Luque and van Beek* [1976]: $q_b^* = 5.7(\tau^* - \tau_c^*)^{1.5}$, and *Wong and Parker* [2006]: $q_b^* = 4.93\ (\tau^* - \tau_c^*)^{1.6}$. We compared results from both versions using a τ_c^* derived from the standard Shields curve for the surface D_{50}. A third MPM analysis on flume data only used the version by *Wong and Parker* [2006], but on specific size fractions, calculating a separate τ_{ci}^* and q_i^* for each phi-size bin, weighted by the percent fraction in the sediment feed.

[43] Predicted transport rates from both MPM models are within one standard deviation of measured rates for the flume and 2001 field data, with the *Wong and Parker* [2006] closer to measured rates; however, both versions overestimate the 1997–1998 transport data by a significant amount. Splitting the calculation into individual size fractions led to an even greater overprediction of the flume transport (Figure 10). The EH model does well if all data are combined, but the results are skewed with the high τ^* transport overestimated and the low τ^* transport underestimated.

5. Discussion

5.1. Bed Development

[44] Both the Pasig-Potrero River and the flume experiments show a transition from a completely sand dominated, unstructured bed surface to a coarser, more organized bed. The driving force behind the transition in our experiments is a reduction in sand input, showing that sand depletion alone can create bed coarsening, clustering, and armor patch development. On the Pasig-Potrero River, it is a reduction in sand input combined with an overall reduction in

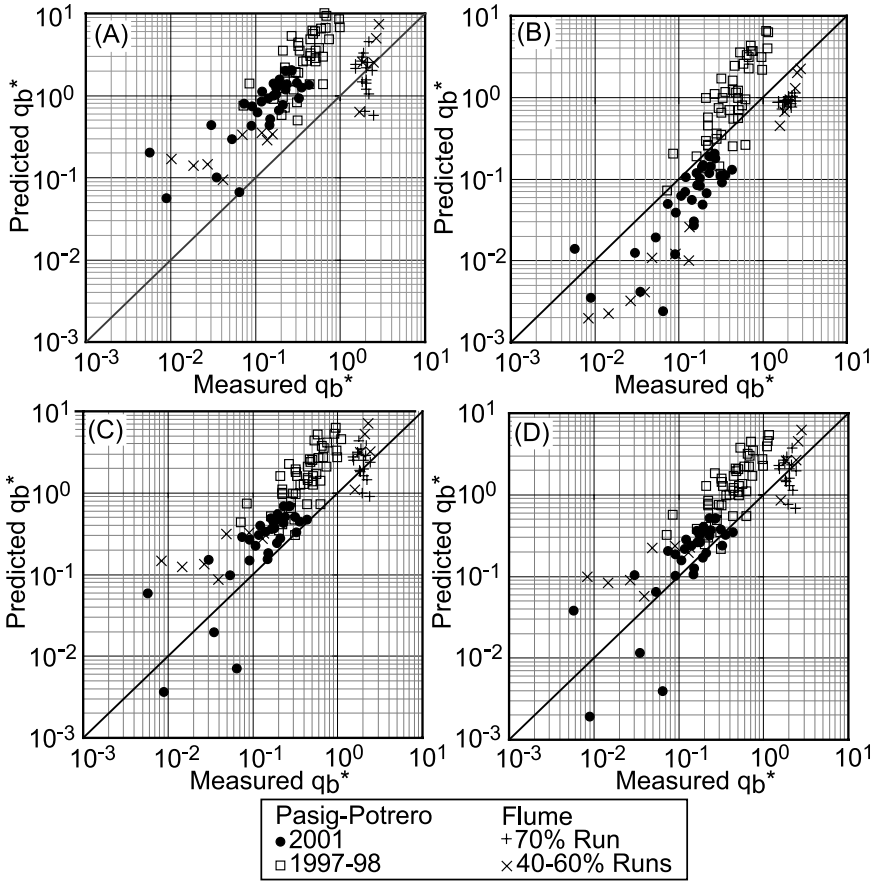

Figure 9. Bed load transport model results showing measured versus predicted transport rates for four different models: (a) two-phase surface-based model of *Wilcock and Kenworthy* [2002]; (b) the relation of *Engelund and Hansen* [1967]; (c) *Meyer-Peter and Müller* [1948] relation as modified by *Fernandez-Luque and van Beek* [1976]; and (d) *Meyer-Peter and Müller* [1948] relation as modified by *Wong and Parker* [2006].

sediment load. However, even with the overall decrease in annual sediment yield, the bed was still transport-limited and aggrading during the time of sampling in 2001.

[45] In our experiments, as sand declined from 70% to 60%, bed coarsening was accommodated through formation of pebble clusters, some of which merged to form weak armor patches. From 60% to 50% sand, distinct armor patches developed, leaving a smooth sand ribbon able to maintain high transport rates. As the percentage of sand declined further, there was not enough sand to maintain the smooth transport zone, and gravel jams began disrupting the longitudinal connectivity of the sand ribbon. The gravel jams became more dominant as sand inputs declined to 40%. In the 40% run, the bed surface had only 32% sand, consistent with the transition between sand-dominated and gravel-dominated transport as measured by *Wilcock et al.* [2001] and *Ikeda and Iseya* [1988].

[46] The Pasig-Potrero River is on a similar trajectory although sand contents in 2001 were still higher in low-flow bed load and on the surface (70% and 39%, respectively) than in the lowest sand run. Following the cessation of major lahars in 1997, the rainy season bed of the Pasig-Potrero River has developed an increasing density of clast structures and armor patches, particularly on low bar complexes within the active braid plain and at the edge of major braids. Similar to bimodal reaches on other rivers [*Sambrook Smith*, 1996], the bed of the Pasig-Potrero River sorted into distinctly bimodal grain size patches (Figure 2). At the alluvial fan head in 2002, sandy transport zones running between armor patches still dominated the bed area. Even if equal mobility of grains is maintained within each patch, the overall effect may be enhanced transport of sand, leading to longitudinal sorting and downstream fining [*Paola and Seal*, 1995]. Strong downstream fining has been observed on the Pasig-Potrero River in the latter half of the 1990s [*Gran and Montgomery*, 2005].

[47] Given the sand content on the bed surface (39%), the bimodal grain size distribution, and the observed development of grain size patchiness at the Delta 5 site, this reach should be nearing the threshold between sand-dominated and transitional transport that we observed in our experiments. Reaches >5 km upstream of Delta 5 cross that threshold during the dry season, when sediment inputs to the main stem channel are reduced. Selective transport winnows the bed during this transition, leading to depletion of sand from the surface. The end result is incision coupled with bed armoring and greatly reduced sediment mobility. The main driving force behind dry season incision is a sharp reduction in sediment supply, and these observations are consistent with experimental studies [*Dietrich et al.*, 1989;

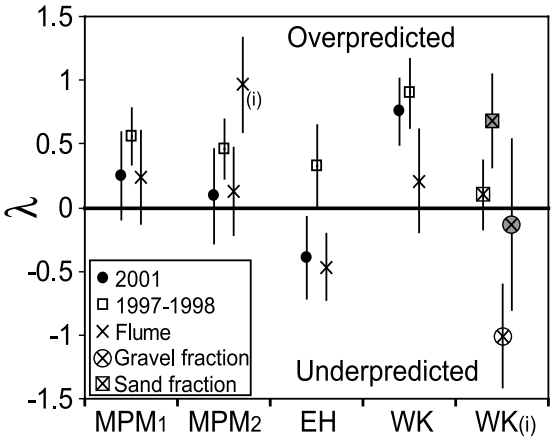

Figure 10. Comparison of the ability of transport models to predict bed load transport rates under a wide range of grain size mixture conditions. Here $\lambda = \log_{10} q_{b(pred)} - \log_{10} q_{b(meas)}$ measures the goodness-of-fit of bed load transport results shown in Figure 9: WK results are shown in Figure 9a, EH in Figure 9b, MPM1 in Figure 9c, and MPM2 in Figure 9d (letter (i) refers to the results from binning MPM2). WK(i) shows the goodness-of-fit of the *Wilcock and Kenworthy* [2002] model for q^*_{bi} for individual sand and gravel fractions in the 70% run (open symbols) and the 40–60% sand runs (shaded symbols).

Lisle et al., 1993]. Other volcanically loaded rivers like the O'Donnell River at Mount Pinatubo and the North Fork Toutle River at Mount St. Helens show a similar shift from multiple-thread, highly mobile channels in the rainy season to single-thread, incised and armored channels in the dry season throughout the watershed [*Gran and Montgomery*, 2005]. Armored reaches on the Pasig-Potrero River form predominantly in the upper basin, but are extending farther downstream as sediment sources are depleted or stabilized.

5.2. Sediment Transport

[48] How does the development of bed structure affect sediment transport? The development of clast structures and armor patches from a previously unarmored bed should increase bed roughness and lower effective shear stress. In addition, as the density of coarse particles on the bed increases, they could form a greater topographic barrier to motion, increasing the friction angle on the bed. Either of these effects may reduce sediment transport rates for a given basal shear stress. We found that reorganization of bed structure into armor patches and sandy ribbons allows the flow to maintain high transport rates while accommodating bed coarsening down to ~40% sand on the bed surface. High transport rates in the flume were also maintained by an increase in slope, which can occur in the field but over a much longer timescale.

[49] On the Pasig-Potrero River, armor patches and zones with a high density of pebble clusters had lower gravel mobility compared to major braids [*Gran and Montgomery*, 2005]. Although clast structures delay entrainment, their main effect on total sediment transport rates may be to narrow the width of low-flow active transport. A delay in entrainment probably has little effect on high-flow transport rates which drive overall sediment yields. Almost all clasts were mobile once fully submerged in unarmored braids.

[50] In our flume experiments, sand ribbons remained highly active, transporting the bulk of the sediment load as coarse patches formed. Abundant sand tends to enhance transport of both sand and gravel. Organization into flow-parallel patches helped maintain high transport rates even as armor developed and the bed coarsened overall. As sand content declined, gravel jams formed in the sand ribbon and bed load was transported in sheets rather than as a continuous strip of moving sediment.

[51] If the entire wetted width of the flume is considered, Manning's n and α' values more than doubled as sand content dropped from 70% to 40% (Tables 2 and 4). If only the active transport zone is considered, analogous to considering only the major braids on the Pasig-Potrero River, we find little effect of the decreasing sand content on parameters affecting sediment transport. Considering only the high-transport zones, we find minimal change in roughness, and α' varied little from 60% down to 40% sand.

[52] Despite our field and flume conditions being highly mobile and sediment-rich, many existing bed load transport models still overpredict transport rates. Interestingly, the updated MPM by *Wong and Parker* [2006] best predicted total bed load transport even though it was designed for uniform sediment over a plane bed. The WK model, which is specifically designed for gravel and sand mixtures, overpredicted total transport rates in all field conditions and flume runs except for the 70% sand run. The benefit of the MPM model is that it is remarkably simple, and it is reassuring that it did such a good job predicting total transport rates over such a wide range of conditions; however, it can predict bulk transport rates only. The WK model offers the ability to predict fractional transport rates, but with more limited accuracy.

[53] Although MPM was able to predict bed load transport rates within one standard deviation for the flume and 2001 field data, WK overpredicted transport rates, EH was skewed, and all models overpredicted the 1997–1998 field data. What can be done to improve either the models or the predictions made with them? Much of the improvement in model prediction lies in improving inputs. For instance, models like MPM were developed under plane bed conditions, but in the field, conditions ranged from plane bed to breaking antidunes, which can change the bed roughness locally by a factor of 2–3 [*Simons and Richardson*, 1966]. Shear stress dissipated by form drag can be substantial in many basins. On the Pasig-Potrero River, the main type of form drag was antidunes, and they would need to dissipate an average of 42% of the total basal shear stress in 1997–1998 for predicted rates using MPM to match measured rates. Considering that breaking antidunes generally occupied <10% of the flow area, this estimate is probably too high to account for the entire discrepency, but shear stress partitioning would improve predicted rates. Other improvements to inputs include better assessment of variations in sediment density with discharge or shear stress (particularly important in the Pasig-Potrero River in 1997–1998) and better in-field measurements in general.

5.3. Current and Future Conditions on the Pasig-Potrero River

[54] Immediately following a volcanic eruption like that at Mount Pinatubo, rivers often convey extremely high

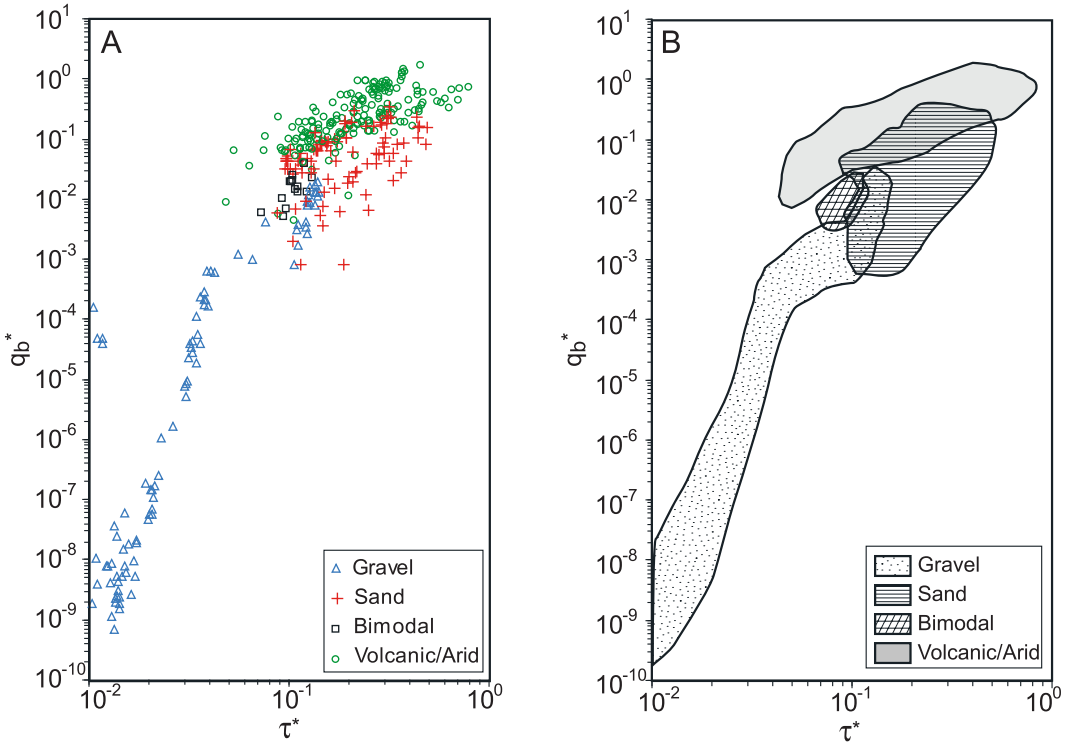

Figure 11. Dimensionless bed load transport (q_b^*) and dimensionless shear stress (τ^*) for the Pasig-Potrero River [*Hayes et al.*, 2002] as compared with other world rivers [*Milhous*, 1973; *Leopold and Emmett*, 1976; *Emmett et al.*, 1985; *Gomez and Church*, 1988; *Pitlick*, 1992; *Reid et al.*, 1995], as modified from *Hayes et al.* [2002]. Here rivers are plotted based on river type (gravel (triangles), sand (plus signs), bimodal (squares), and volcanic/arid ephemeral (circles)). Figure 11a shows the data, and Figure 11b summarizes the general range covered by each river type.

sediment loads [*Kadomura et al.*, 1983; *Pearson*, 1986; *Hirao and Yoshida*, 1989; *Umbal*, 1997; *Dinehart*, 1998; *Major et al.*, 2000; *Tuñgol*, 2002; *Major*, 2004]. Even following the cessation of major lahars, some volcanic rivers maintain high transport for decades [*Major et al.*, 2000; *Major*, 2004]. *Hayes et al.* [2002] demonstrated that for a given τ^*, low-flow q_b^* rates on the Pasig-Potrero River were an order of magnitude higher than transport rates on the sand-bedded East Fork River in Wyoming [*Emmett et al.*, 1985], and were similar to those measured during flash floods on the Nahal Yatir, an arid ephemeral stream [*Reid et al.*, 1995]. *Hayes et al.* [2002] also compared the Pasig-Potrero River to the volcanically loaded North Fork Toutle River, Washington, and gravel-bedded Oak Creek, Oregon. We extend this comparison to include five additional rivers: three gravel-bedded rivers, one sand-bedded river, and one bimodal braided river (Figure 11).

[55] Sand-dominated and gravel-dominated rivers occupy two different regions on the plot, with the bimodal braided Tanana River in between. Bed load transport rates on volcanic and arid rivers are 1–2 orders of magnitude higher than transport rates on sand-bedded rivers for the same τ^*. This may be due to a higher overall supply on these channels or to a higher supply of gravel in an otherwise sand-dominated system. It could also be due to higher transport rates in these mostly unarmored systems. Supercritical flow was common in all three arid or volcanic channels during storm events, and was common on the Pasig-Potrero River even during low-flow. Experiments have shown that coarse pebbles and cobbles have much greater mobility over a sandy bed at supercritical flow than under subcritical flow conditions [*Fahnestock and Haushild*, 1962], so supercritical flow in these flash-flood and volcanically loaded systems could lead to enhanced gravel transport.

[56] Future sediment yields at Mount Pinatubo will depend on inputs from remaining deposits of sand-rich eruptive material. As sand inputs decline, the transport regime is shifting toward the region occupied by bimodal and gravel-bedded channels. The flume data show the same shift toward the gravel transport regime with decreasing sand content. Already, seasonal patterns in sediment inputs on the Pasig-Potrero River are reflected in the changing bed structure and sediment transport rates between the rainy season and the dry season. The shift to transitional and even to gravel-dominated transport may already be occurring during the dry season, lowering bed load transport rates. The timescale for the transition from sand-dominated to gravel-dominated transport during the rainy season will depend primarily on the rate of sand depletion in the upper basin.

6. Conclusions

[57] As sand inputs decline, bed reorganization into flow-parallel patches helps maintain high transport rates while accommodating bed coarsening on the Pasig-Potrero River. Bed partitioning allows roughness, critical shear stress, and grain size distributions to remain fairly constant in sandy

transport zones over a wide range of grain size mixtures. Once sand inputs fall to the point that gravel jams clog the sandy transport zone, the sediment transport regime will shift from sand-dominated to transitional, slowing transport rates. In our experiments, the shift from sand-dominated to transitional transport occurred at bed surface sand contents consistent with those measured by *Ikeda and Iseya* [1988] and *Wilcock et al.* [2001]. In 2001, sand contents on the bed surface of the Pasig-Potrero River (39% sand) were nearing the transitional range during the rainy season, but transport remained sand-dominated in major unarmored braids. Despite the wide range of sand and gravel mixtures in both field and flume, transport rates under most conditions were predicted well using a modified version of the standard *Meyer-Peter and Müller* [1948] model by *Wong and Parker* [2006].

[58] Because the channel bed tends to sort into armor patches prior to development of full bed armor, significant bed coarsening can be accommodated with minimal impact on sediment transport as long as sand ribbons remain connected. Patch development thus compresses the transition from sand to gravel into a narrow range of sand content rather than a continuous, smooth transition over a wide range of sand content. This effect could help explain why, in general, most channels are sand-bedded or gravel-bedded, with fewer bimodal or transitional channels, and why transitional reaches are relatively short even in channels with downstream gravel to sand transitions.

[59] **Acknowledgments.** This work was supported by a grant from the U.S. National Science Foundation (EAR-0106681). K. Gran was supported through a graduate fellowship from the U.S. Environmental Protection Agency's Science to Achieve Results (STAR) program. We would like to thank the students and staff at Humboldt State University and the U.S. Forest Service's Redwood Sciences Laboratory for assistance with the flume experiments. Many thanks to Tom Lisle for helpful discussions and to Chris Newhall for invaluable assistance throughout this project. For assistance and logistical support in the field, we thank PHIVOLCS (Philippine Institute for Volcanology and Seismology) and particularly the staff at the Pinatubo Volcano Observatory. Thanks also to Cristina Hoff, Tim Cook, Boy Tanglao, and Talosa Tanglao, who helped with the sediment sampling in 2001. Comments and discussions with Jeff Parsons and Derek Booth helped improve this manuscript.

References

Beverage, J. P., and J. K. Culbertson (1964), Hyperconcentrations of suspended sediment, *J. Hydraul. Div. Am. Soc. Civ. Eng.*, *90*, 117–128.

Brayshaw, A. C. (1984), Characteristics and origin of cluster bedforms in coarse-grained alluvial channels, in *Sedimentology of Gravels and Conglomerates*, edited by E. H. Koster and R. J. Steel, pp. 77–85, Can. Soc. of Pet. Geol., Calgary, Alberta, Canada.

Buffington, J. M., W. E. Dietrich, and J. W. Kirchner (1992), Friction angle measurements on a naturally formed gravel streambed: Implications for critical boundary shear stress, *Water Resour. Res.*, *28*, 411–425.

Church, M., M. A. Hassan, and J. F. Wolcott (1998), Stabilizing self-organized structures in gravel-bed stream channels: Field and experimental observations, *Water Resour. Res.*, *34*, 3169–3179.

Daag, A. S. (1994), Geomorphic developments and erosion of the Mount Pinatubo 1991 pyroclastic flows in the Sacobia watershed, Philippines: A study using remote sensing and geographic information systems (GIS), M.S. thesis, 106 pp., Int. Inst. for Geoinf. Sci. and Earth Obs., Enschede, Netherlands.

Daag, A. S. (2003), Modelling the erosion of pyroclastic flow deposits and the occurrences of lahars at Mt. Pinatubo, Philippines, Ph.D. thesis, 232 pp., Int. Inst. for Geoinf. Sci. and Earth Obs., Enschede, Netherlands.

Dietrich, W. E., J. W. Kirchner, H. Ikeda, and F. Iseya (1987), The origin of the coarse surface layer in gravel-bedded streams: The role of sediment supply, *Geol. Soc. Am. Abstr. Programs*, *19*, 642.

Dietrich, W. E., J. W. Kirchner, H. Ikeda, and F. Iseya (1989), Sediment supply and the development of the coarse surface layer in gravel-bedded rivers, *Nature*, *340*, 215–217.

Dinehart, R. L. (1998), Sediment transport at gauging stations near Mount St. Helens, Washington, 1980–90: Data collection and analysis, *U.S. Geol. Surv. Prof. Pap.*, *1573*, 105 pp.

Edwards, T. K., and G. D. Glysson (1999), Field methods for measurement of fluvial sediment, *U.S. Geol. Surv. Tech. Water Resour. Invest. Rep.*, *3–C2*, 89.

Emmett, W. W., R. M. Myrick, and R. H. Martinson (1985), Hydraulic and sediment-transport data, East Fork River, Wyoming, 1978, *U.S. Geol. Surv. Open File Rep.*, *85–486*, 37.

Engelund, F., and E. Hansen (1967), *A Monograph on Sediment Transport in Alluvial Streams*, 62 pp., Teknisk, Copenhagen.

Fahnestock, R. K., and W. L. Haushild (1962), Flume studies of the transport of pebbles and cobbles on a sand bed, *Geol. Soc. Am. Bull.*, *73*, 1431–1436.

Ferguson, R. I. (2003), Emergence of abrupt gravel to sand transitions along rivers through sorting processes, *Geology*, *31*, 159–162.

Ferguson, R. I., K. L. Prestegaard, and P. J. Ashworth (1989), Influence of sand on hydraulics and gravel transport in a braided gravel bed river, *Water Resour. Res.*, *25*, 635–643.

Fernandez-Luque, R., and R. van Beek (1976), Erosion and transport of bedload sediment, *J. Hydraul. Res.*, *14*(2), 127–144.

Gilbert, G. K. (1917), Hydraulic mining debris in the Sierra Nevada, *U.S. Geol. Surv. Prof. Pap.*, *105*, 154.

Gomez, B., and M. Church (1988), A catalogue of equilibrium transport data for coarse sand and gravel-bed channels, 90 pp., Univ. of B. C., Vancouver, B. C., Canada.

Gran, K. B. (2005), Fluvial recovery from basin-wide sediment loading at Mount Pinatubo, Philippines, Ph.D. thesis, 203 pp., Univ. of Washington, Seattle.

Gran, K. B., and D. R. Montgomery (2005), Spatial and temporal patterns in fluvial recovery following volcanic eruptions: Channel response to basin-wide sediment loading at Mount Pinatubo, Philippines, *Geol. Soc. Am. Bull.*, *117*, 195–211, doi:10.1130/B25528.1.

Hayes, S. K. (1999), Low-flow sediment transport on the Pasig-Potrero alluvial fan, Mount Pinatubo, Philippines, M.S. thesis, 73 pp., Univ. of Washington, Seattle.

Hayes, S. K., D. R. Montgomery, and C. G. Newhall (2002), Fluvial sediment transport and deposition following the 1991 eruption of Mount Pinatubo, *Geomorphology*, *45*, 211–224.

Hirao, K., and M. Yoshida (1989), Sediment yield of Mt. Galunggung after eruption in 1982, in paper presented at the International Symposium on Erosion and Volcanic Debris Flow Technology, Yogyakarta, Indonesia, 31 July to 3 Aug.

Ikeda, H., and F. Iseya (1988), Experimental study of heterogeneous sediment transport, *Rep. 12*, 50 pp., Environ. Res. Cent., Univ. of Tsukuba, Tsukuba, Japan.

Iseya, F., and H. Ikeda (1987), Pulsations in bedload transport rates induced by a longitudinal sediment sorting: A flume study using sand and gravel mixtures, *Geogr. Ann., Ser. A*, *69*, 15–27.

Kadomura, H., T. Imagawa, and H. Yamamoto (1983), Eruption-induced rapid erosion and mass movements on Usu volcano, Hokkaido, *Z. Geomorphol. Suppl.*, *46*, 123–142.

Kirchner, J. W., W. E. Dietrich, F. Iseya, and H. Ikeda (1990), The variability of critical shear stress, friction angle, and grain protrusion in water-worked sediments, *Sedimentology*, *37*, 647–672.

Knighton, A. D. (1989), River adjustment to changes in sediment load: The effects of tin mining on the Ringarooma River, Tasmania, 1875–1984, *Earth Surf. Processes Landforms*, *14*, 333–359.

Knighton, A. D. (1991), Channel bed adjustment along mine-affected rivers of northeast Tasmania, *Geomorphology*, *4*, 205–219.

Knighton, A. D. (1999), The gravel-sand transition in a disturbed catchment, *Geomorphology*, *27*, 325–341.

Kodama, Y. (1994), Experimental study of abrasion and its role in producing downstream fining in gravel-bed rivers, *J. Sediment. Res.*, *64*, 76–85.

Koster, E. H. (1978), *Transverse Ribs: Their Characteristics, Origin, and Paleohydraulic Significance*, pp. 161–186, Can. Soc. of Pet. Geologists, Calgary, Alberta, Canada.

Kuhnle, R. A., and J. B. Southard (1988), Bed load transport fluctuations in a gravel bed laboratory channel, *Water Resour. Res.*, *24*, 247–260.

Leopold, L. B., and W. W. Emmett (1976), Bedload measurements, East Fork River, Wyoming, *Proc. Natl. Acad. Sci. U. S. A.*, *73*, 1000–1004.

Lisle, T. E. (1995), Particle size variations between bed load and bed material in natural gravel bed channels, *Water Resour. Res.*, *31*, 1107–1118.

Lisle, T. E., F. Iseya, and H. Ikeda (1993), Response of a channel with alternate bars to a decrease in supply of mixed-size bed load: A flume experiment, *Water Resour. Res.*, *29*, 3623–3629.

Madej, M. A., and V. Ozaki (1996), Channel response to sediment wave propagation and movement, Redwood Creek, California, USA, *Earth Surf. Processes Landforms*, *21*, 911–927.

Maita, H. (1991), Sediment dynamics of a high gradient stream in the Oi River Basin of Japan, *Gen. Tech. Rep. PSW, PSW-GTR-130*, pp. 56–64.

Major, J. J. (2004), Posteruption suspended sediment transport at Mount St. Helens: Decadal-scale relationships with landscape adjustments and river discharges, *J. Geophys. Res.*, *109*, F01002, doi:10.1029/2002JF000010.

Major, J. J., R. J. Janda, and A. S. Daag (1996), Watershed disturbance and lahars on the east side of Mount Pinatubo during the mid-June 1991 eruptions, in *Fire and Mud: Eruptions and Lahars of Mount Pinatubo, Philippines*, edited by C. G. Newhall and R. S. Punongbayan, pp. 895–919, Philippine Inst. of Volcanol. and Seismol., Quezon City, Philippines.

Major, J. J., T. C. Pierson, R. L. Dinehart, and J. E. Costa (2000), Sediment yield following severe volcanic disturbance—A two-decade perspective from Mount St. Helens, *Geology*, *28*, 819–822.

Meyer-Peter, E., and R. Müller (1948), Formulas for bed-load transport, paper presented at the 2nd Meeting of the International Association for Hydraulic Structures Research, Stockholm, Sweden.

Milhous, R. T. (1973), Sediment transport in a gravel-bottomed stream, Ph.D. thesis, 232 pp., Oreg. State Univ., Corvallis.

Montgomery, D. R., M. S. Panfil, and S. K. Hayes (1999), Channel-bed mobility response to extreme sediment loading at Mount Pinatubo, *Geology*, *27*, 271–274.

Needham, D. J., and J. H. Merkin (1984), On roll waves down an open inclined channel, *Proc. R. Soc. London A*, *394*, 259–278.

Paola, C., and R. Seal (1995), Grain size patchiness as a cause of selective deposition and downstream fining, *Water Resour. Res.*, *31*, 1395–1407.

Paola, C., G. Parker, R. Seal, S. K. Sinha, and J. B. Southard (1992), Downstream fining by selective deposition in a laboratory flume, *Science*, *258*, 1757–1760.

Pearson, M. L. (1986), Sediment yields from the debris avalanche for water years 1980–1983, in *Mount St. Helens: Five Years Later*, edited by S. A. C. Keller, pp. 87–107, East. Wash. Univ. Press, Spokane.

Pickup, G. (1984), Geomorphology of tropical rivers: 1. Landforms, hydrology, and sedimentation in the Fly and lower Purari, Papua New Guinea, *Catena Suppl.*, *5*, 1–17.

Pitlick, J. (1992), Flow resistance under conditions of intense gravel transport, *Water Resour. Res.*, *28*, 891–903.

Reid, I., J. B. Laronne, and D. M. Powell (1995), The Nahal Yatir bedload database: Sediment dynamics in a gravel-bed ephemeral stream, *Earth Surf. Processes Landforms*, *20*, 845–857.

Sambrook Smith, G. H. (1996), Bimodal fluvial bed sediments: Origin, spatial extent and processes, *Prog. Phys. Geogr.*, *20*, 402–417.

Sambrook Smith, G. H., and R. I. Ferguson (1995), The gravel-sand transition along river channels, *J. Sediment. Res., Sect. A*, *65*, 423–430.

Scott, W. E., R. P. Hoblitt, R. C. Torres, S. Self, M. M. L. Martinez, and T. Nillos (1996), Pyroclastic flows of the June 15, 1991, climactic eruption of Mount Pinatubo, in *Fire and Mud: Eruptions and Lahars of Mount Pinatubo, Philippines*, edited by C. G. Newhall and R. S. Punongbayan, pp. 545–570, Philippine Inst. of Volcanol. and Seismol., Quezon City, Philippines.

Seal, R., and C. Paola (1995), Observations of downstream fining on the North Fork Toutle River near Mount St. Helens, Washington, *Water Resour. Res.*, *31*, 1409–1419.

Shaw, J., and R. Kellerhals (1982), The composition of recent alluvial gravels in Alberta river beds, *Alberta Res. Counc. Bull.*, *41*, 151 p.

Simons, D. B., and E. V. Richardson (1966), Resistance to flow in alluvial channels, *U.S. Geol. Surv. Prof. Pap.*, *422J*, J1–J61.

Tuñgol, N. M. (2002), Lahar initiation and sediment yield in the Pasig-Potrero River basin, Mount Pinatubo, Philippines, Ph.D. thesis, 172 pp., Univ. of Canterbury, Christchurch, New Zealand.

Umbal, J. V. (1997), Five years of lahars at Pinatubo volcano: Declining but still potentially lethal hazards, *J. Geol. Soc. Philipp.*, *52*, 1–19.

Whiting, P. J., W. E. Dietrich, L. B. Leopold, T. G. Drake, and R. L. Shreve (1988), Bedload sheets in heterogeneous sediment, *Geology*, *16*, 105–108.

Wilcock, P. R., and S. T. Kenworthy (2002), A two-fraction model for the transport of sand/gravel mixtures, *Water Resour. Res.*, *38*(10), 1194, doi:10.1029/2001WR000684.

Wilcock, P. R., and B. W. McArdell (1993), Surface-based fractional transport rates: Mobilization thresholds and partial transport of a sand-gravel sediment, *Water Resour. Res.*, *29*, 1297–1312.

Wilcock, P. R., S. T. Kenworthy, and J. C. Crowe (2001), Experimental study of the transport of mixed sand and gravel, *Water Resour. Res.*, *37*, 3349–3358.

Wittenberg, L. (2002), Structural patterns in coarse gravel rivers beds: Typology, survey and assessment of the roles of grain size and river regime, *Geogr. Ann.*, *84*, 25–37.

Wolcott, J. F. (1988), Non-fluvial control of bimodal grain size distributions in river bed gravels, *J. Sediment. Petrol.*, *58*, 979–984.

Wolman, M. G. (1954), A method of sampling coarse river-bed material, *Eos Trans. AGU*, *35*(6), 951–956.

Wong, M., and G. Parker (2006), Re-analysis and correction of bedload relation of Meyer-Peter and Muller using their own database, *J. Hydraul. Eng.*, in press.

Yatsu, E. (1955), On the longitudinal profile of the graded river, *Eos Trans. AGU*, *36*(4), 655–663.

K. B. Gran, National Center for Earth-Surface Processes, St. Anthony Falls Laboratory, University of Minnesota, 23rd Avenue SE, Minneapolis, MN 55414, USA. (kgran@umn.edu)

D. R. Montgomery, Department of Earth and Space Sciences, University of Washington, Seattle, WA 98195, USA.

D. G. Sutherland, U.S. Forest Service Pacific Southwest Research Station, Redwood Sciences Laboratory, Arcata, CA 95521, USA.